

The solution of (7) has been given by Clarke [2] as

$$\psi_2 = (\sqrt{2})f_1(\infty)(x^2 + y^2)^{3/2} \sin \left\{ \frac{3}{4} \tan^{-1} \left(\frac{y}{x} \right) + \frac{\pi}{4} \right\}, \quad (8)$$

which may be compared with [1], equation (24). Kierkus in fact, in his outer solution, attempts to model the effects of a finite plate whilst retaining the solution for a semi-infinite plate in the inner region. His first-order inner and outer solutions are therefore incompatible. The finite-plate problem remains unsolved.

Returning now to the next term of the inner solution we consider (1b) for the pressure distribution. With $P_2 = x^2 h_2(\eta)$ we have for the upper surface

$$h_2' = g_1 \tan \phi, \quad h_2 \rightarrow 0 \quad \text{as} \quad \eta \rightarrow \infty. \quad (9)$$

This has been given by Kierkus as the leading term of a series associated with the second-order boundary-layer solution. However we note that the remaining terms in his series are meaningless within the context of the incompatibility of his first-order solutions. As Kierkus notes, the pressure distribution in the boundary layer which forms on the lower surface is obtained from (9) by simply changing the sign of ϕ . As for the symmetrical case $\phi = 0$ (see [2]) it can be shown that $\Theta_2 \equiv 0$. The second-order velocity field Ψ_2 within the boundary layer adjusts the "slip" velocity $\partial\psi_2/\partial y|_{y=0} = \frac{3}{4}x^{-4}f_1(\infty)$, ($x > 0$) to zero at the plate; its structure is significantly influenced by the self induced pressure field calculated from (9). Thus if we write $\Psi_2 = f_{2\pm}(\eta)$ where \pm refer to the upper and lower sides of the plate respectively, then from (1a)

$$\left. \begin{aligned} f_{2\pm}'' + \frac{3}{4}f_1 f_{2\pm}' - \frac{1}{4}f_1' f_{2\pm} \mp (h_2 - \eta h_2') &= 0, \\ f_{2\pm}(0) = f_{2\pm}'(0) &= 0, \quad f_{2\pm}(\infty) = \frac{3}{4}f_1(\infty). \end{aligned} \right\} \quad (10)$$

This solution has also been given by Kierkus, as the leading term of an otherwise meaningless series. We show in Fig. 1 the velocity functions $f_{2\pm}'(\eta)$ for $\sigma = 1$, $\phi = 60^\circ$. The asymmetry in the boundary-layer flow brought about by the favourable/adverse pressure gradients on the upper/lower surfaces is clearly demonstrated. To calculate the next term in

the outer series (3) we require a matching condition which is derived from the asymptotic form of the solution of (10) as $\eta \rightarrow \infty$. Thus $f_{2\pm} \sim \frac{3}{4}f_1(\infty)\eta + c_{2\pm}$ as $\eta \rightarrow \infty$ where, for $\sigma = 1$, $\phi = 60^\circ$, $c_{2+} = 6.7845$, $c_{2-} = -11.2985$. Before proceeding we make the following important observation, namely that $f_2 = \frac{1}{2}(f_{2+} + f_{2-})$ is the solution in the absence of any self-induced pressure field, i.e. $\phi = 0$ as in [2]. Thus if $f_2 \sim \frac{3}{4}f_1(\infty)\eta + c_2$ then

$$c_2 = \frac{1}{2}(c_{2+} + c_{2-}). \quad (11)$$

If we now consider the term $O(Gr^{-1/2})$ in (3), it can again be established that the solution is isothermal and irrotational, so that the problem for ψ_3 is

$$\nabla^2 \psi_3 = 0, \quad \psi_3 = \pm c_{2\pm}, \quad y = 0 \pm, \quad x > 0. \quad (12)$$

The solution of (12) for ψ_3 is

$$\psi_3 = c_2 + \frac{1}{2\pi}(c_{2+} + c_{2-}) \tan^{-1} \left(\frac{y}{x} \right), \quad (13)$$

from which the purely symmetrical solution is obtained by setting $c_{2\pm} = c_2$. However since the streamlines in the outer flow are given by $\psi = \text{const.}$ we see from (8), (11) and (13) that to an observer outside the boundary layer the symmetrical streamline pattern associated with the case $\phi = 0$ is preserved. Only the 'label' associated with each streamline is changed by the constant amount $\frac{1}{2}(c_{2+} - c_{2-})$. Streamlines calculated from (8), the leading term in (3), are shown in [2]. In Fig. 2 we show the effect upon the streamline pattern of including the second term (13), for a particular value of Gr .

We note finally that since $\Theta_2 \equiv 0$ the heat transfer from the plate is the same as that for a vertical plate up to, but not including, terms of relative order $Gr^{-1/2}$.

REFERENCES

1. W. T. Kierkus, *Int. J. Heat Mass Transfer* **11**, 241 (1968).
2. J. F. Clarke, *J. Fluid Mech.* **57**, 45 (1973).
3. D. R. Jones, *Q. Jl Mech. appl. Math.* **26**, 77 (1973).

Int. J. Heat Mass Transfer. Vol. 18, pp. 993-996. Pergamon Press 1975. Printed in Great Britain

EFFECT OF LIGHTER NONCONDENSABLE GAS ON LAMINAR FILM CONDENSATION OVER A VERTICAL PLATE

ORAN RUTUNAPRAKARN* and CHING JEN CHEN†

Energy Division, College of Engineering, The University of Iowa, Iowa City, Iowa 52242, U.S.A.

(Received 17 May 1974 and in revised form 5 December 1974)

NOMENCLATURE

C_p ,	specific heat at constant pressure;
$f(\eta)$,	normalized stream function;
g ,	gravity;
h_x ,	local heat-transfer coefficient;
k ,	thermal conductivity;
M ,	molecular weight;
Nu_x ,	local Nusselt number;
Pr ,	Prandtl number;
Sc ,	Schmidt number;
T ,	temperature;
u, v ,	x and y components of velocity;
W ,	mass fraction;
x, y ,	parallel and normal direction to the wall.

Greek symbols

λ ,	latent heat;
ρ ,	density;
β_T ,	coefficient of expansion;
μ ,	viscosity;
θ ,	dimensionless temperature;
ϕ ,	dimensionless concentration;
ζ ,	ratio of the product of density and viscosity;
η ,	similarity variable.

Subscripts and superscripts

1,	condensable vapor;
2,	noncondensable gas;
L ,	liquid;
V ,	vapor;
i ,	interface;
∞ ,	bulk;

*Research Assistant.

†Associate Professor.

w, wall;
 N, Nusselt model;
 (), differentiation.

INTRODUCTION AND ANALYSIS

It is well known [1-3] that the presence of noncondensable gases in a vapor can substantially decrease the heat-transfer rate in film condensation. Many analyses [4-6] were done for the case in which the noncondensable gas has a larger molecular weight than that of the vapor. When the molecular weight of the noncondensable gas is smaller or lighter than that of the condensable there will be an unfavorable buoyancy effect which tends to retard the flow of vapor condensing on a vertical wall. Spencer *et al.* [7] experimented with Freon 12 mixed separately with lighter gases of nitrogen, helium, and carbon dioxide and found that a large reduction of heat transfer occurred in the presence of very small amount of noncondensable gas and that the lighter the noncondensable gas, the stronger the instability of the vapor-liquid interface will be. In this note similarity solutions of film condensation, under unfavorable buoyancy condition with small percentage of noncondensable gas are given.

Consider an isothermal vertical flat plate at temperature T_w is immersed in a large bulk of a gas-vapor mixture at a saturated temperature T_∞ . When the film condensate flows downward along the plate, y coordinate, due to gravity, the gas vapor mixture is induced to move by the condensed liquid and by the natural convection resulting from temperature and concentration gradients of the mixture. The local concentrations of vapor and gas can be expressed as $W_1 = \rho_1/\rho_v$ and $W_2 = \rho_2/\rho_v$ where ρ_v is the local density of the mixture and ρ_1 and ρ_2 are the local densities of the vapor and gas. When the mixture is assumed as an ideal gas and the Boussinesq and boundary layer approximation are used the equations expressing conservation of mass, momentum and energy for the laminar film condensation can be found elsewhere [4, 5] or [8].

Under similarity transformation [8] the similarity variables for liquid and vapor side, subscripted with, L , and V , respectively are

$$\eta_L = C_L y/x^{\frac{1}{2}} \quad C_L = \left[\frac{g(\rho_L - \rho_\infty)}{4\nu_L^2 \rho_L} \right]^{\frac{1}{2}}$$

$$\eta_V = C_V y_V/x^{\frac{1}{2}} \quad C_V = \left[\frac{g|\beta_T|(W_{1\infty} - W_{1i})}{4\nu_V^2} \right]^{\frac{1}{2}}$$

The temperature, concentration and velocity components in terms of the above similarity variables are

$$\theta_L(\eta_L) = \frac{T_L - T_i}{T_w - T_i} \quad \phi = \frac{W_1 - W_{1\infty}}{W_{1i} - W_{1\infty}}$$

$$u_L = 4\nu_L C_L^2 x^{\frac{1}{2}} f_L' \quad u_V = 4\nu_V C_V^2 x^{\frac{1}{2}} f_V'$$

$$v_L = \nu_L C_L x^{-\frac{1}{2}} (\eta_L f_L' - 3f_L) \quad v_V = \nu_V C_V x^{-\frac{1}{2}} (\eta_V f_V' - 3f_V)$$

The governing equations under the similarity transformation become

$$f_L''' + 3f_L f_L'' - 2f_L'^2 + 1 = 0$$

$$\theta_L'' + 3Pr_L f_L \theta_L' = 0$$

$$f_V''' + 3f_V f_V'' - 2f_V'^2 + \text{sign}(\beta_T)\phi = 0$$

$$\phi'' + 3Sc f_V \phi' = 0$$

where

$$\beta_T = -\frac{1}{\rho_\infty} \left(\frac{\partial \rho_V}{\partial W_1} \right)_{T_\infty} = (M_2 - M_1) / [(M_2 - M_1)W_{1\infty} + M_1]$$

$$\text{sign}(\beta_T) = \begin{cases} +1 & \text{for } \beta_T > 0 \text{ or } M_2 > M_1 \\ & \text{(heavier noncondensable)} \\ -1 & \text{for } \beta_T < 0 \text{ or } M_2 < M_1 \\ & \text{(lighter noncondensable)} \end{cases}$$

M denotes the molecular weight while Pr_L and Sc are respectively the Prandtl and Schmidt number. W_{1i} is the vapor concentration at the interface.

The boundary conditions under the similarity transformation are: at the wall, $\eta_L = 0$: $f_L = 0$, $f_L' = 0$, $\theta_L = 1$; at the liquid-vapor interface, $\eta_L = \eta_{L\delta}$ or $\eta_V = 0$: $\theta_L = 0$, $\phi = 0$; at the edge of vapor boundary layer, $\eta_V \rightarrow \infty$: $f_V' = 0$, $\phi = 0$.

The interfacial matching conditions under the similarity transformations [8] are:

$$\text{Interface velocity: } f_V' = \xi^{-\frac{1}{2}} f_{Vi}' \quad \zeta = \frac{\rho_L \mu_L}{\rho_V \mu_V}$$

$$\text{Interface mass flow: } f_V = \xi^{\frac{1}{2}} \xi^{-\frac{1}{2}} f_{Vi} \quad \xi = |\beta_T|(W_{1\infty} - W_{1i})$$

$$\text{Interface shear stress: } f_V'' = \xi^{\frac{1}{2}} \xi^{-\frac{1}{2}} f_{Vi}''$$

The interfacial temperature T_i and concentration W_{1i} are given as

$$C_{pL}(T_i - T_w) = \frac{-3Pr_L f_L(\eta_{L\delta})}{\lambda \theta_L'(\eta_{L\delta})}$$

$$W_{1i} = \frac{W_{1\infty} \phi'(\eta_V = 0) + 3Sc f_V(\eta_V = 0)}{\phi'(\eta_V = 0) + 3Sc f_V'(\eta_V = 0)}$$

The heat transfer at the wall is then obtained as

$$\frac{h_x x}{k_L} = Nu_x = - \left[\frac{g(\rho_L - \rho_\infty) x^3}{4\rho_L \nu_L^2} \right]^{\frac{1}{2}} \theta_L'(0) \frac{(T_i - T_w)}{(T_\infty - T_w)}$$

Since the heat transfer of the pure vapor under Nusselt's assumption is

$$Nu_{xN} = \left[\frac{C_{pL}(T_\infty - T_w) 4\nu_L k_L}{\lambda g C_{pL}(\rho_L - \rho_\infty) x^3} \right]^{-\frac{1}{2}}$$

the ratio of the present heat-transfer coefficient to that of Nusselt may be considered as an estimate of the effect of the noncondensable gas on heat transfer.

RESULTS AND DISCUSSION

We choose a mixture Freon-12 vapor with N_2 as a lighter noncondensable for computation because of its practical importance in the refrigeration process. Numerical solutions were carried out mostly for Schmidt number of $Sc = 0.3$ but sufficient solutions were also obtained for $Sc = 0.2$ to indicate the trend when temperature ranges are varied (Tables 1 and 2).

In the present calculation, the latent heat, λ , is evaluated at T_∞ while the value of C_{pL} and Pr_L are evaluated at $T_w + 0.31(T_\infty - T_w)$.

Table 1. Numerical solutions of the vapor governing equations

Run No.	Sc	$f_V(0)$	$f_V'(0)$	$f_V''(0)$	$\phi(0)$
1	0.3	1.75	0.6	-3.8966	-1.62682
2	0.3	2.00	0.6	-4.2597	-1.85062
3	0.3	3.00	0.6	-5.8534	-2.74034
4	0.3	5.00	0.6	-9.2780	-4.52638
5	0.3	1.50	0.3	-2.1527	-1.35042
6	0.3	2.00	0.3	-2.3805	-1.81664
7	0.3	5.00	0.3	-4.7351	-4.51267
8	0.3	3.00	1.0	-9.6140	-2.76985
9	0.2	3.00	0.6	-6.0342	-1.82456
10	0.2	5.00	0.6	-9.3874	-3.01806
11	0.2	2.00	0.3	-3.2746	-1.80805
12	0.2	5.00	0.3	-4.8462	-3.00792
13	0.5	0.80	0.050	0.5190	-1.30590
14	0.5	1.35	0.050	0.2600	-2.06380
15	0.5	0.50	0.145	0.4220	-0.97244
16	0.5	1.20	0.145	-0.0451	-1.87277

Runs 1 to 12 are for Freon 12-nitrogen case (lighter noncondensable).

Runs 13 to 16 are for steam-air case (heavier noncondensable).

Table 2. Sample data of heat-transfer calculation ($Sc = 0.3$) for Freon 12-nitrogen mixture

Run No.	$W_{1\infty}$	W_{1i}	ζ	$f_L(V_{1\infty})$	$f_L(V_{1i})$	η_{L0}	T_{∞}	T_i	$\theta(0)$	$\frac{C_{pL}(T_i - T_w)}{\lambda Pr_L}$	T_w	Nu_x
1	0.9999	0.9968	38.39	0.0145	0.0614	0.3344	59.17	58.27	-2.833	0.161	45.84	0.9515
1	0.9995	0.9843	15.97	0.0524	0.1372	0.5570	142.18	136.50	-1.843	0.104	79.16	0.9538
2	0.9999	0.9963	40.48	0.0164	0.0664	0.3691	54.77	53.80	-2.722	0.0202	38.97	0.9563
2	0.9995	0.9817	16.65	0.0597	0.1484	0.5847	138.82	132.30	-1.765	0.1270	60.84	0.9660
3	0.9999	0.9932	43.63	0.0268	0.0911	0.4366	48.13	46.32	-2.311	0.0381	16.59	0.9630
3	0.9995	0.9660	16.38	0.1067	0.2036	0.7354	140.10	128.25	-1.468	0.3000	-59.49	1.0225
4	0.9999	0.9828	43.20	0.0569	0.1455	0.5724	49.04	44.56	-1.795	0.1020	-44.07	0.9655
5	0.9998	0.9287	59.55	0.0590	0.1484	0.5803	48.93	41.60	-1.773	0.0902	-103.93	0.8542
6	0.9998	0.9781	45.83	0.0228	0.0819	0.4135	43.51	38.16	-2.436	0.0903	13.60	0.8702
7	0.9998	0.9920	17.36	0.0698	0.1632	0.6189	135.50	132.69	-1.6918	0.4867	43.46	1.0094

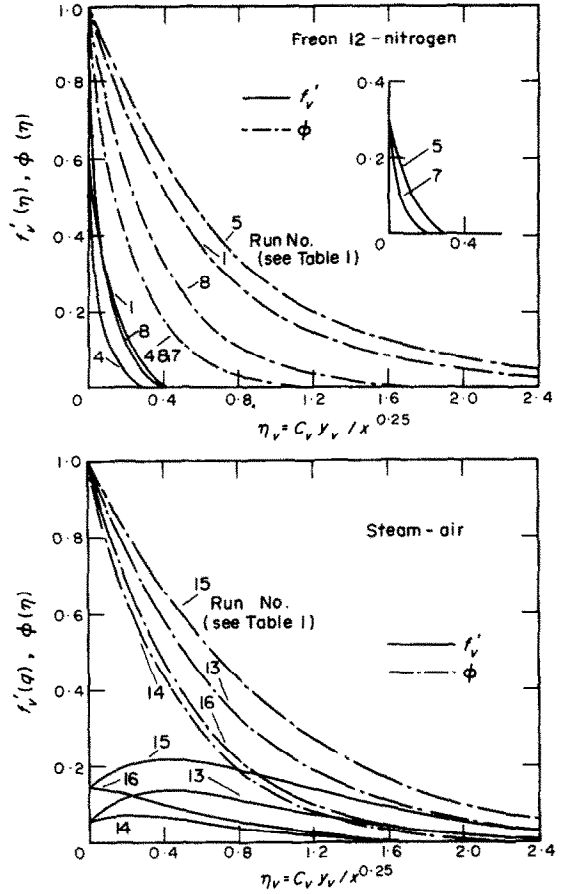


FIG. 1. Velocity and concentration profiles.

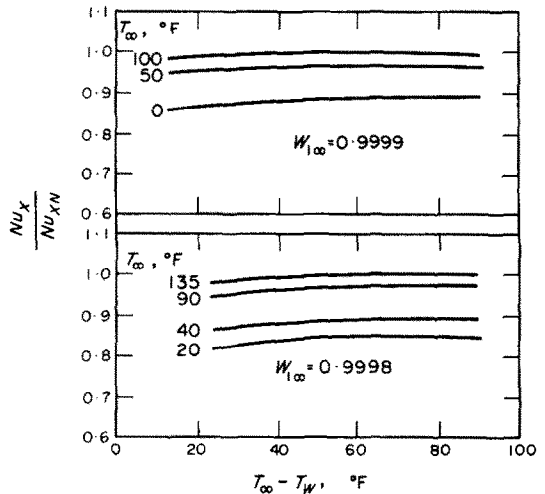


FIG. 2. Heat-transfer result for Freon 12-nitrogen mixture.

Figure 1 shows typical vapor velocity and concentration profiles for the mixture of Freon 12-nitrogen. We note that the thickness of the velocity boundary layer is smaller than that of concentration layer. This is partially due to the buoyant force which tends to move nitrogen gas upward and hence to retard the downflow of Freon-12 vapor and liquid. As a result although the mixture moves downward it moves slower than the case of pure vapor. Thus nitrogen accumulates near the interface to build up a large concentration layer. In addition, the fact that Schmidt number of Freon 12-nitrogen mixture is less than unity,

means that the mass diffusivity is larger than the viscous diffusivity. Therefore, the concentration layer should be larger than the velocity layer. In order to bring out the contrast of the effect of lighter and heavier noncondensable gas we calculated several cases of steam-air mixture as also shown in Fig. 1. From the figure we see that while the concentration profile for steam-air mixture is similar to the Freon 12-nitrogen mixture, the velocity profiles are distinctly different. First the velocity boundary layer thickness is much larger for the steam-air mixture because of a larger value of Schmidt number 0.5, and the favorable

buoyant effect. Secondly the interfacial shear is smaller and in many instances the shear force acts in the opposite direction compared with the Freon 12–nitrogen mixture (see Table 1 for $f_v''(0)$). Furthermore the fact that the buoyant effect introduces a larger shear force at the interface for the case of Freon 12–nitrogen mixture may promote instability in both the vapor boundary layer and the liquid–vapor interface as pointed out by the experimental work of Spencer *et al.* [7]. They observed the instability of the vapor boundary layer while operating on a saturated bulk temperature from 80 to 100°F and a temperature difference between the bulk and the wall being about 2–36°F with a mass fraction of the condensable vapor in the bulk form 0.993 or less. Two heat-transfer results are shown in Fig. 2. It is seen that the presence of a small amount of non-condensable gas in the bulk may cause a considerable reduction in heat transfer such that a presence of 0.01 per cent of nitrogen in Freon 12 vapor operating at 0°F may cause a reduction in heat transfer more than 10 per cent. It is noted that as the pressure (temperature) at which condensation process takes place decreases, the effect of noncondensable gas in reducing heat transfer increases. This trend is observed in steam–air system studied by Minkowycz and Sparrow [5]. Physically, when the operating pressure (temperature) decreases, the mixture density decreases. Therefore, the ratio of $(\rho\mu)_L/(\rho\mu)_V$ increases. As a consequence, the interfacial concentration of noncondensable gas increases and thus causes a reduction in heat transfer. In general, in the case of Freon 12–nitrogen mixture, numerical results show that the temperature drop in the liquid phase is more pronounced than that in the vapor phase. For example (Table 2), when the operating temperature, T_∞ , is at 48.1°F with $Sc = 0.3$, $W_{1,\infty} = 0.9999$, we obtain $T_i = 46.3°F$ when $T_w = 16.6°F$. On the contrary, the trend is generally opposite in the case of steam–air mixture.

As an example [8], we have $T_\infty = 200°F$ with $Sc = 0.5$, $W_{1,\infty} = 0.98$ then $T_i = 180.8°F$ when $T_w = 177.3°F$. It should be remarked finally that similarity solution does not exist for high bulk concentration of noncondensable gas in the case of lighter noncondensable.

REFERENCES

1. H. Hampson, *Proceedings of the General Discussion on Heat Transfer*, Vol. 84, pp. 58–61. Institution of Mechanical Engineers, London, and American Society of Mechanical Engineers, New York (1951).
2. L. Slegers and R. A. Seban, Laminar film condensation of steam containing small concentrations of air, *Int. J. Heat Mass Transfer* **13**, 1941–1946 (1970).
3. H. K. Al-Diwany and J. W. Rose, Free convection film condensation of steam in the presence of non-condensing gases, *Int. J. Heat Mass Transfer* **16**, 1359–1369 (1973).
4. E. M. Sparrow and S. H. Lin, Condensation heat transfer in the presence of a noncondensable gas, *J. Heat Transfer* **86**, 430–436 (1964).
5. W. J. Minkowycz and E. M. Sparrow, Condensation heat transfer in the presence of noncondensable, interfacial resistance, superheating, variable properties and diffusion, *Int. J. Heat Mass Transfer* **9**, 1125–1144 (1966).
6. J. W. Rose, Condensation of a vapour in the presence of a non-condensing gas, *Int. J. Heat Mass Transfer* **12**, 233–237 (1969).
7. D. L. Spencer, K. I. Chang and H. C. Moy, Experimental investigation of stability effects in laminar film condensation on a vertical cylinder, *Heat Transfer 1970*, Vol. 6, Chapter 2.3, pp. 1–11 (1970).
8. O. Rutunaprakarn, Effects of noncondensable gas with different molecular weight on laminar film condensation, M. S. Thesis, Department of Mechanical Engineering, The University of Iowa (May 1973).

GRAETZ PROBLEM IN CURVED RECTANGULAR CHANNELS WITH CONVECTIVE BOUNDARY CONDITION—THE EFFECT OF SECONDARY FLOW ON LIQUID SOLIDIFICATION-FREE ZONE

K. C. CHENG, RAN-CHAU LIN and JENN-WUU OU

Department of Mechanical Engineering, University of Alberta, Edmonton, Alberta, Canada

(Received 17 May 1974 and in revised form 27 November 1974)

NOMENCLATURE

Bi ,	Biot number, hD_e/k ;
D_e ,	equivalent hydraulic diameter, $2ab/(a+b)$;
h ,	heat-transfer coefficient,
	$-k(\partial T/\partial N)_w = h(T_w - T_\infty)$;
K ,	Dean number, $Re(D_e/R)^{1/2}$;
k ,	thermal conductivity;
N ,	outward normal at wall;
Nu ,	local Nusselt number, hD_e/k ;
n ,	dimensionless outward normal, N/D_e ;
Pr ,	Prandtl number, ν/α ;
R ,	radius of curvature;
Re ,	Reynolds number, $D_e \bar{W}/\nu$;
r ,	dimensionless radius of curvature, R/D_e ;
T, T_f, T_0, T_∞ ,	fluid temperature, freezing temperature of liquid, uniform fluid entrance temperature and ambient fluid temperature, respectively;
U, V, W ,	velocity components in X, Y, Z directions;

\bar{W} ,	average axial velocity;
u, v, w ,	dimensionless velocity components,
	$[(U, V)/(v/D_e), W/\bar{W}]$;
X, Y, Z ,	Cartesian coordinates;
x, y, z ,	dimensionless coordinates,
	$[(X, Y)/D_e, Z/D_e(PrRe)]$;
z_f ,	dimensionless entrance distance where solidification begins;
γ ,	aspect ratio of a rectangular channel, b/a ;
ϵ ,	superheat ratio, $(T_0 - T_f)/(T_f - T_\infty)$;
θ ,	dimensionless temperature difference,
	$(T - T_\infty)/(T_0 - T_\infty)$;
θ_b, θ_w ,	bulk temperature,
	$\iint_A \theta w dx dy / \iint_A w dx dy$,
	and local wall temperature;
ψ ,	dimensionless stream function [12, 13];
$\bar{\quad}$,	average quantity.